Chemical Behavior and in Vitro Activity of Mixed Phosphine Gold(I) Compounds on Melanoma Cell Lines

Francesco Caruso,*[,†] Claudio Pettinari,*[,‡] Francesco Paduano,[△] Raffaella Villa,[△] Fabio Marchetti,[‡] Elena Monti,[⊥] and Miriam Rossi[§]

Istituto di Chimica Biomolecolare, Consiglio Nazionale delle Ricerche (CNR), c/o University of Rome Istituto Chimico, Piazzale Aldo Moro 5, 00185, Rome, Italy, Dipartimento di Scienze Chimiche, Università di Camerino, via S. Agostino 1, 62032 Camerino, MC, Italy, Department of Chemistry, Vassar College, Poughkeepsie, New York 12604-0484, U.O. 10, Dipartimento Sperimentale, Fondazione IRCCS "Istituto Nazionale dei Tumori", Via Venezian 1, 20133 Milan, Italy, and Dipartimento di Biologia Strutturale e Funzionale, Università dell'Insubria, Via A. da Giussano, 12, 21052 Busto Arsizio,VA, Italy

Received August 6, 2007

^{31}P nuclear magnetic resonance and electrospray ionization−mass spectrometry studies on the melanoma cytotoxic chlorotriphenylphosphine-1,3-bis(diphenylphosphino)propanegold(I), [Au(DPPP)(PPh_3)Cl], show partial decomposition that includes the novel dinuclear cation $[Au_2(DPPP)_2Cl]^+$; its structure was calculated by using the density functional theory (DFT). Unexpectedly, by using the diphosphine ligand 1,2-bis(diphenylphosphino)ethane (DIPHOS), [{AuCl(PPh_3)}$_2$(μ_2-DIPHOS)] was obtained. Its X-ray crystal structure shows a unique triangular coordination sphere in contrast to the T-shaped geometry of related Au(I)−DIPHOS compounds. Its cytotoxic activity in JR8, SK-Mel-5, and 2/60 melanoma cell lines is dose-dependent and lower than that of [Au(DPPP)(PPh_3)Cl] because of its nonchelating nature. An in vitro study of the effect of both Au compounds on the B16V melanoma cell line gives credence to this structure−activity relationship. IC_{50} indicates that both Au species are 10 times more active in B16V than in JR8, SK-Mel-5, and 2/60. Oxidation of [Au(DPPP)(PPh_3)Cl] toward Au(III) compounds and phosphine−oxides is observed upon reaction with hypochlorite in water/dimethyl sulfoxide solution, mimicking endogenous hypochlorite. A related reaction involving the formation of $[AuCl_4]^-$ is thermodynamically feasible according to DFT calculations.

Introduction

There is much interest in the research on metal complexes as potential anticancer agents. Clinical use of cisplatin has induced an ongoing investigation of alternative metal-based anticancer agents, in the hope that metal centers other than platinum might produce specific and/or improved in vitro and in vivo anticancer effects and be developed as useful drugs.[1,2] The clinically established antiarthritic Au(I) species auranofin (1-thio-betaβ-D-glucopyranosato)(triethylphosphine)gold 2,3,4,6-tetraacetate) and some other Au−phosphine compounds show significant antitumor properties, both in vitro and in vivo.[3,4] Au(I) complexes containing diphosphine ligands show the greatest antitumor activity in vitro and in vivo in P388 and L1210 leukemias, M5076 reticulum cell sarcoma, B16 melanoma, and Lewis lung carcinoma.[5–8]

The site where Au(I)−monophosphine and −diphosphine complexes act is in mitochondria. Here, they cause uncoupling of oxidative phosphorylation, altering the inner mitochondrial membrane permeability to cations and protons, causing the consequent collapse of the mitochondrial membrane potential ($\Delta\psi_{mt}$).[9–13] The antitumor activity may be due to loss of $\Delta\psi_{mt}$, which results in decreased ATP synthesis and release of apoptogenic factors from the mitochondria into the cytosol, leading to cell death.[14,15] Interest in the design and development of drugs that specifically compromise the structural and functional integrity of mitochondria is growing.[16–18]

To potentially increase antitumor activity through synergistic effects, the Au(I) complex chlorotriphenylphosphine-1,3-bis-(diphenylphosphino)propanegold(I), [Au(DPPP)(PPh_3)Cl][a], containing both mono- and diphosphine ligands, was recently synthesized. It showed appreciable in vitro antiproliferative activity against the National Cancer Institute 60-cell-line panel derived from tumors of different histotypes; melanoma was the most sensitive subgroup analyzed,[19] and thus, we focus on this tumor type. Such selectivity has been recently confirmed on additional human melanoma cell lines (JR8, SK-Mel-5, Mel-501, 2/60, 2/21, and GRIG), and the cytotoxic activity was higher than or comparable to that of cisplatin.[20] Additionally, apoptotic response of JR8 and 2/60 cells exposed to [Au-(DPPP)(PPh_3)Cl] showed a dose-dependent loss of mitochondrial membrane potential, release of cytochrome *c* and Smac/DIABLO from the mitochondria into the cytosol, and a dose-dependent increase in apoptotic cells.[20] Activity of Au complexes with chelating ligands $PPh_2(CH_2)_nPPh_2$ is higher for $n = 2$, 3, and therefore, we attempted to synthesize the analogous mixed phosphine compound [Au(DIPHOS)(PPh_3)Cl], that is, a complex containing a $-[(CH_2)_2]_2-$ link instead of $-[(CH_2)_2]_3-$ between the two PPh_2 units, to test its influence on biological activity. We obtained an unexpected Au−DIPHOS species, and we describe below the antiproliferative effect of this novel compound on three human melanoma cell lines, JR8, SK-Mel-5,

* Corresponding authors. Phone: 39 06 499136. Fax: 39 06 49913628. E-mail: caruso@vassar.edu. Phone: 39 0737 402234. Fax: 39 0737 637345. E-mail: claudio.pettinari@unicam.it.

† Consiglio Nazionale delle Ricerche (CNR).

‡ Università di Camerino.

△ Fondazione IRCCS "Istituto Nazionale dei Tumori".

⊥ Università dell'Insubria.

§ Vassar College.

[a] Abbrevations: [Au(DPPP)(PPh_3)Cl], chlorotriphenylphosphine-1,3-bis-(diphenylphosphino)propanegold(I); DPPP, 1,3-bis(diphenylphosphino)propane; DIPHOS, 1,2-bis(diphenylphosphino)ethane; DMPP, 1,3-bis(dimethylphosphino)propane; NMR, nuclear magnetic resonance; ESI-MS, electrospray ionization−mass spectrometry; DMSO, dimethyl sulfoxide.

10.1021/jm700978a CCC: $40.75 © 2008 American Chemical Society
Published on Web 02/29/2008

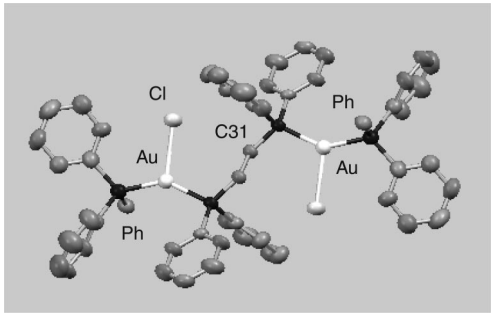

Figure 1. X-ray crystal structure of [{AuCl(PPh$_3$)}$_2$(μ_2-DIPHOS)] showing ellipsoid displacement parameters. For two Ph groups only, the *ipso* carbons are shown, and all H atoms are omitted for clarity. P, black; C, gray; Au, white; and Cl, light gray. The inversion center of this molecule is located in the ethylene bridge between C31 and C31′.

Table 1. Selected Structural Parameters of [{AuCl(PPh$_3$)}$_2$(μ_2-DIPHOS)]

	X-ray	DFT
Au−P(Ph) (Å)	2.313(4)	2.483
Au−P(DIPHOS) (Å)	2.323(4)	2.485
Au−Cl (Å)	2.632(5)	2.538
P(DIPHOS)−Au−P(Ph) (°)	145.2(2)	131.0
Cl−Au−P(Ph) (°)	108.9(2)	115.9
Cl−Au−P(DIPHOS) (°)	105.8(2)	113.0

and 2/60. We also include additional studies in solution by using nuclear magnetic resonance (NMR) and electrospray ionization−mass spectrometry (ESI-MS) and outline differences between [Au(DPPP)(PPh$_3$)Cl] and the Au−DIPHOS complexes, including the novel Au species [Au$_2$(DPPP)$_2$Cl]$^+$, studied with the density functional theory (DFT). An additional in vitro study was performed for both metal compounds on a murine melanoma in vitro cell line (B16V) derived from the in vivo transplanted B16 melanoma.

Results

Diffraction Study of [{AuCl(PPh$_3$)}$_2$(μ_2-DIPHOS)]. The X-ray crystal structure of [{PPh$_3$AuCl}$_2$(μ_2-DIPHOS)] is depicted in Figure 1 and shows a nonchelating DIPHOS ligand bridging two Au centers. A solvent chloroform molecule is included in the lattice and does not show chemical interactions with [{AuCl(PPh$_3$)}$_2$(μ_2-DIPHOS)]. Therefore, the Au center is 3-coordinate, that is, bound to one Cl and two P atoms, one from PPh$_3$ and one from DIPHOS, and its coordination polyhedron is triangular. Table 1 lists selected structural features for both X-ray and DFT methods, which are described later.

A literature search for Au−DIPHOS chelate, with 3-coordinate metal, shows only three compounds in the Cambridge crystallographic database, whereas there are 13 crystal structures for DIPHOS-bridged Au species with at least one Au atom 3-coordinate. Therefore, having a nonchelate 3-coordinate Au(I)−DIPHOS compound appears statistically favorable. Most of these molecules have ring-like connectivity, and the Au coordination geometry is T-shaped, although sometimes ring constraints induce distortions; all have less triangular character than [{AuCl(PPh$_3$)}$_2$(μ_2-DIPHOS)]. Nine out of the 13 compounds show interactions between both Au atoms as well. The most direct comparison is made with the only Cl derivative, (μ_2-2,3-bis(diphenylphosphino)-1,3-butadiene-P,P′)-dichlorodigold(I),[21] which has a T-shaped Au geometry with one Au−Cl (bond length 2.30 Å) and two Au−P (bond length about 2.24 Å). The Au coordination sphere of [{AuCl(PPh$_3$)}$_2$(μ_2-DIPHOS)], besides being different because it is triangular, has weaker Au−P bonds (2.313(4) Å to PPh$_3$ and 2.323(4) Å to DIPHOS). This suggests a poor Au-protecting capacity by DIPHOS in [{AuCl(PPh$_3$)}$_2$(μ_2-DIPHOS)], which is confirmed because most Au−P(DIPHOS) bond lengths in the 13 structures mentioned above are generally much shorter, see Figure 2.

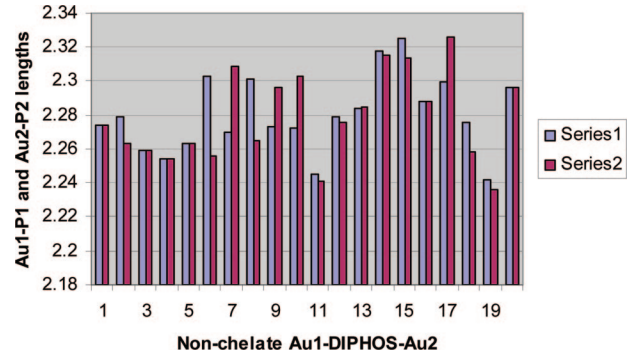

Figure 2. Graph of 13 nonchelate Au(I)−DIPHOS crystal structures found at the Cambridge Structural Database (listed in the Supporting Information); some of these species have more than one independent molecular unit.

Chemistry. Crystalline [{AuCl(PPh$_3$)}$_2$(μ_2-DIPHOS)] was obtained by mixing in 1:1 molar ratio chloroform solutions of chlorotriphenylphosphinegold(I), [Au(PPh$_3$)Cl], and DIPHOS. In contrast, an equivalent process using DPPP in dichloromethane instead of DIPHOS yielded [Au(DPPP)(PPh$_3$)Cl] as previously described.[19] [{AuCl(PPh$_3$)}$_2$(μ_2-DIPHOS)] is air- and moisture-stable and has been fully characterized by spectroscopic methods (IR, NMR, and ESI-MS). Its IR spectrum shows the bands due to the phosphine ligands to be close to those of analogous phosphine−Au(I) complexes.[22,23] A weak band at ca. 320 cm^{-1} likely corresponds to ν(Au−Cl) vibration.[23–25] Its ^{31}P{^{1}H} NMR spectrum, recorded at room temperature in CDCl$_3$, shows three signals that can be assigned to different phosphorus environments. In the ESI-MS spectrum, signals are associated with ionic species, and it is only with this technique that we could observe the formation of a species, [Au(DIPHOS)(PPh$_3$)]$^+$, closely related to the one originally wanted. The reaction between [Au(PPh$_3$)Cl] and DIPHOS in acetonitrile was monitored with the same technique. When excess DIPHOS was employed, [Au(DIPHOS)$_2$]$^+$ was the only cation detected in solution; when equimolar quantities were used, two cations, [Au(PPh$_3$)$_2$]$^+$ and [Au(DIPHOS)$_2$]$^+$, were found to coexist, and when an excess of [Au(PPh$_3$)Cl] was used, the signals due to [(PPh$_3$)(DIPHOS)Au]$^+$, [(PPh$_3$)(DIPHOS)Au$_2$Cl]$^+$, and [(PPh$_3$)$_2$(DIPHOS)Au$_2$Cl]$^+$ appeared, the latter increasing with the increase in [Au(PPh$_3$)Cl] concentration.

The ^{31}P{^{1}H} NMR spectrum of [Au(DPPP)(PPh$_3$)Cl], in CDCl$_3$ and dimethyl sulfoxide (DMSO), showed the existence of the following products: [Au(DPPP)(PPh$_3$)Cl], [Au(DPPP)$_2$]Cl, PPh$_3$, and [Au(PPh$_3$)$_2$Cl]. However, ESI-MS in MeCN indicated the presence of these cations: [Au(DPPP)PPh$_3$]$^+$, [Au(DPPP)$_2$]$^+$, [Au(PPh$_3$)$_2$]$^+$, and [Au$_2$(DPPP)$_2$]Cl$^+$, all of them known except the last one. Therefore, ESI-MS and NMR spectra demonstrate that [Au(DPPP)(PPh$_3$)Cl] undergoes partial dissociation in CHCl$_3$, DMSO, and acetonitrile to give stable and known species, many of them carrying DPPP and the novel cationic species [Au$_2$(DPPP)$_2$]Cl$^+$, described later with DFT methods, see Schemes 1 and 2.

Because recent studies showed that endogenous hypochlorite interacts with Au(I) antiarthritic drugs,[26] we analyzed the hypochlorite oxidation of [Au(DPPP)(PPh$_3$)Cl] to Au(III) and

Scheme 1. Diphosphine Ligands Used in this Work

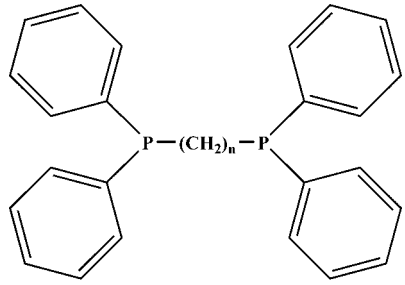

DIPHOS: n = 2; DPPP: n = 3

Scheme 2. Decomposition of [Au(DPPP)(PPh$_3$)Cl]

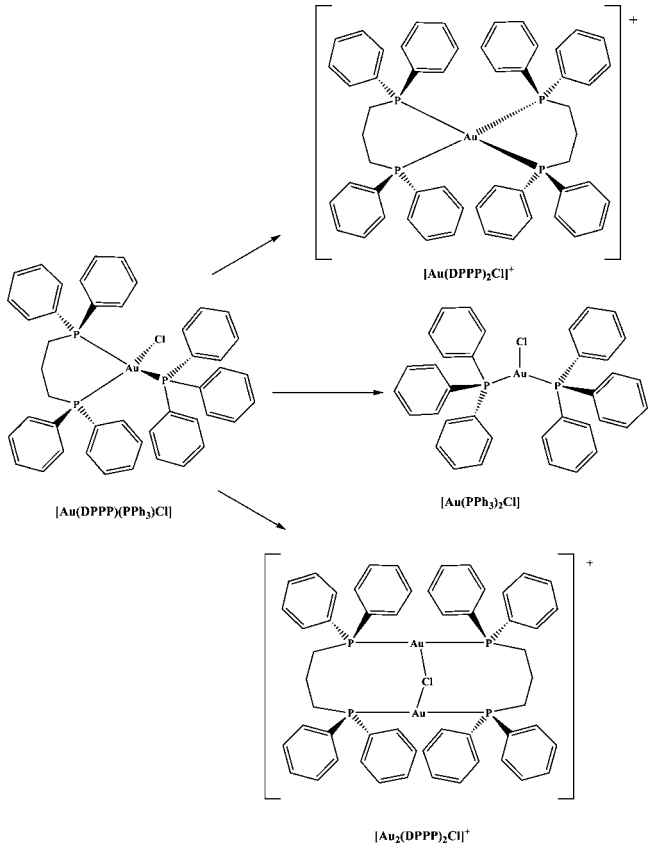

Scheme 3

$$[Au(DPPP)(PPh_3)Cl] \leftrightarrows [Au(DPPP)_2]Cl + [Au(PPh_3)_2Cl]$$

found the formation of several Au(III) species. First, we analyzed [Au(DPPP)(PPh$_3$)Cl] by ^{1}H and ^{31}P{^{1}H}NMR in a water/DMSO solution buffered at physiological pH. Its dissociation toward [Au(DPPP)$_2$]Cl and [Au(PPh$_3$)$_2$Cl] depends on dilution and temperature. Signals due to [Au(DPPP)(PPh$_3$)Cl], [Au(DPPP)$_2$]Cl, and [Au(PPh$_3$)$_2$Cl] are always present. When NaOD was added to the mixture, signals due to PPh$_3$O and DPPPO$_2$ were immediately observed. On the other hand, ^{31}P NMR spectra ($CDCl_3$) of equimolar [Au(DPPP)(PPh$_3$)Cl] and DCl indicate that [Au(DPPP)(PPh$_3$)Cl] persists at low pH values, and the equilibrium shown in Scheme 3 is shifted to the right.

When ClO^- was added to a NMR test tube containing a $CDCl_3$ solution of [Au(DPPP)(PPh$_3$)Cl], several signals appeared immediately. Some were assigned to the following species: [PPh$_3$AuCl$_3$],[27] [(DPPP)AuCl$_2$]Cl, [(PPh$_3$)AuCl], [(DPPP)AuCl], and [Au(DPPP)$_2$]Cl. It is worth noting that, upon

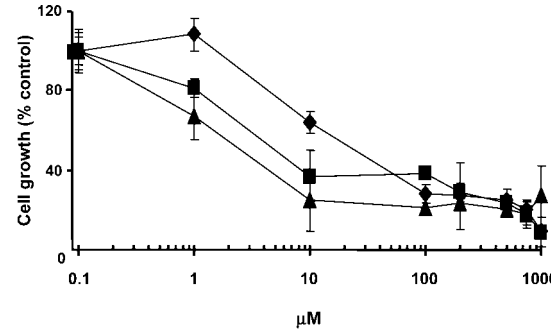

Figure 3. Dose−response curves of human melanoma cell lines (JR8 (■), 2/60 (♦), and SK-MEL-5 (▲)) exposed to [{AuCl(PPh$_3$)}$_2$(μ_2-DIPHOS)] for 48 h. Points represent mean values ± SD of three independent experiments.

Table 2. Cytotoxic Activity of Au Complexes in Human Melanoma Cell Lines

	IC$_{50}$ (μM)[a]	
	[{AuCl(PPh$_3$)}$_2$(μ_2-DIPHOS)]	[Au(DPPP)(PPh$_3$)Cl]
JR8	28 ± 0.33	0.8 ± 0.11
SK-MEL-5	2.7 ± 0.11	1.0 ± 0.56
2/60	5.5 ± 0.085	1.7 ± 0.47

[a] IC$_{50}$ values were determined graphically from the growth inhibition curves obtained after a 48-h exposure of the cells to each drug. Data represent mean values ± SD of three independent experiments. Values for [Au(DPPP)(PPh$_3$)Cl] are taken from the literature.[20]

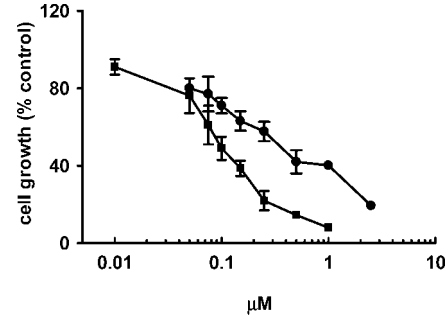

Figure 4. Dose−response curves obtained from B16V cells exposed to [{AuCl(PPh$_3$)}$_2$(μ_2-DIPHOS)] (♦) and [Au(DPPP)(PPh$_3$)Cl] (•) for 48 h. Points represent the mean ± SD of four independent experiments.

ClO^- addition, the solution became yellow, and $[AuCl_4]^-$ was identified by UV spectroscopy.[28]

Acetonitrile/H$_2$O solutions of [Au(DPPP)(PPh$_3$)Cl] and ClO^- have also been investigated by ESI-MS. $[AuCl_4]^-$ and $[AuCl_2]^-$ in 5:1 ratio have been identified in the negative spectrum, whereas, in the positive one, signals due to $[(PPh_3O)_2 + Na]^+$, $[(DPPPO_2)_2 + Na]^+$, $[(PPh_3O)(DPPPO_2) + Na]^+$, $[PPh_3AuCl_2]^+$, $[(DPPP)AuCl_2]^+$, $[(PPh_3)_2Au]^+$, $[(DPPP)(PPh_3)Au]^+$, and $[(DPPP)Au(Cl)(H_2O)]^{2+}$ are present, depending on the dilution of the solution. Upon further addition of ClO^-, the signals due to $[(PPh_3)_2Au]^+$ and $[(DPPP)(PPh_3)Au]^+$ disappear, whereas those due to $[(PPh_3O)_2 + Na]^+$, $[(DPPPO_2)_2 + Na]^+$, $[PPh_3AuCl_2]^+$, and $[(DPPP)AuCl_2]^+$ increase in intensity. When large excess ClO^- is added, signals due to $[PPh_3AuCl_2]^+$ and $[(DPPP)AuCl_2]^+$ also disappear, and the only one present for Au-containing species is due to $[AuCl_4]^-$. By adding PPh$_3$ or DPPP to this solution, $[PPh_3AuCl_2]^+$ and $[(DPPP)AuCl_2]^+$ form again. Finally, addition of a strong excess of PPh$_3$ regenerates PPh$_3$AuCl, as expected.[28] Spectroscopic data therefore suggest that reacting [Au(DPPP)(PPh$_3$)Cl] with ClO^- oxidizes Au(I) to Au(III), as confirmed by the presence of several Au(III)−

Scheme 4. Nonchelate and Chelate Connectivities of $[Au_2(DPPP)_2Cl]^+$

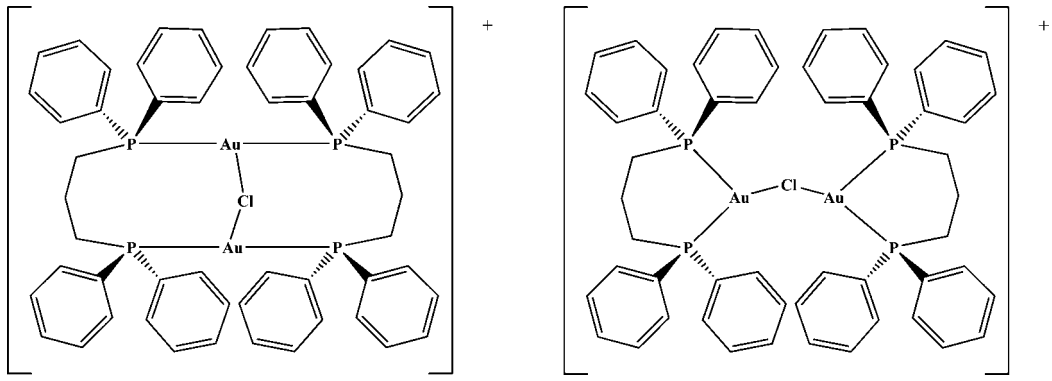

phosphine cations and $[AuCl_4]^-$ in the ESI-MS spectrum. This is also supported by the fact that addition of an equimolar quantity of PPh_3 to the above NMR solution produces PPh_3AuCl_3. The oxidation of Au(I) to Au(III) is accompanied by the oxidation of both phosphine donors to phosphinooxide species.

In conclusion, ^{31}P NMR spectra of chloroform (or D_2O/DMSO) solutions containing [Au(DPPP)(PPh_3)Cl] and ClO^- agree with ESI-MS spectra of acetonitrile solution containing the same species; these are input for DFT calculations also described later.

Cytotoxic Activity. The in vitro cytotoxic activity of the Au complex [{AuCl(PPh_3)}$_2$(μ_2-DIPHOS)] was investigated in JR8, SK-Mel-5, and 2/60 human melanoma cell lines exposed to different concentrations (from 0.1 to 1000 μM) for 48 h. A dose-dependent inhibition of cell growth was observed in all cell lines (Figure 3), with IC_{50} values ranging from 2.7 to 28 μM. This cytotoxic effect was compared to that reported for [Au(DPPP)(PPh_3)Cl][20] under the same experimental conditions (Table 2); the DIPHOS complex was less potent than the DPPP one in inhibiting cell growth. A related study was performed on the B16V murine melanoma cell line for both [Au(DPPP)(PPh_3)Cl] and [{AuCl(PPh_3)}$_2$(μ_2-DIPHOS)]. The dose−response curves obtained for the two compounds are depicted in Figure 4; nonlinear regression analysis gave IC_{50} values of 0.09 ± 0.02 and 0.32 ± 0.08 μM, respectively (mean ± SD of four independent experiments). The difference between the two values is highly statistically significant by Student's t test for independent samples ($p < 0.001$).

Theoretical Calculations. The structural features of $[Au_2(DPPP)_2Cl]^+$ were investigated with DFT. Initial coordinates for a nonchelate arrangement (Scheme 4, left) were obtained after modification of the closely related bis(μ_2-chloro)-bis(μ_2-*R*,*S*-(1-diphenylphosphinobut-2-yl)-diphenylphosphinite)-digold(I) crystal structure,[29] see Figure 5. In addition, an alternative connectivity having two chelating Au(DPPP) moieties linked by the bridging Cl atom was explored (Scheme 4, right). The molecule having the lowest energy showed a Au−Cl−Au moiety typical of aurophilic interaction and is shown in Figure 6. [{PPh_2AuCl}$_2$(μ_2-DIPHOS)] was investigated with DFT technique, because anisotropic crystalline decay was seen during data collection. Initial coordinates from the X-ray structure were geometry-minimized, and the triangular coordination resulting was more regular (see Figure S1).

To study the reactivity of ClO^- toward [Au(DPPP)(PPh_3)Cl], we decreased the calculation time by replacing all Ph groups with methyls in phosphine ligands so that [Au(DPPP)(PPh_3)Cl] was modeled as [Au(DMPP)($PMet_3$)Cl]. When comparing the calculated structures of [Au(DMPP)($PMet_3$)Cl] and its cationic derivative $[Au(DMPP)(PMet_3)]^+$, it is seen that the role of Cl^-

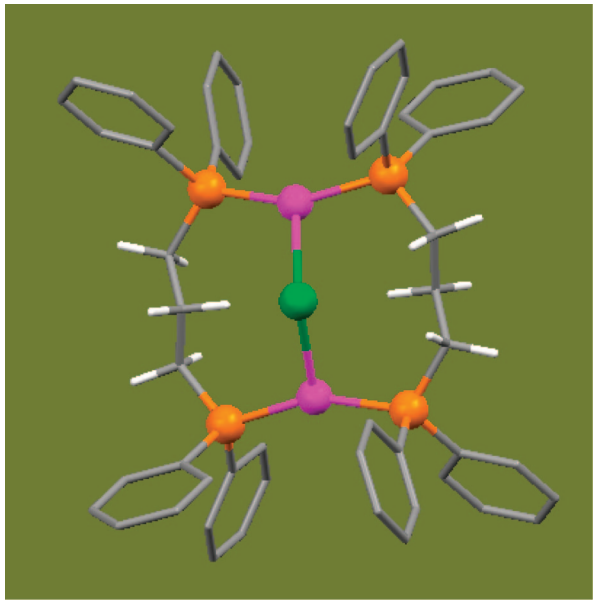

Figure 5. Nonchelate structure of $[Au_2(DPPP)_2Cl]^+$ obtained with DFT methods and having aromatic H atoms omitted for clarity. P, orange; C, gray; H, white; Au, purple; and Cl, green.

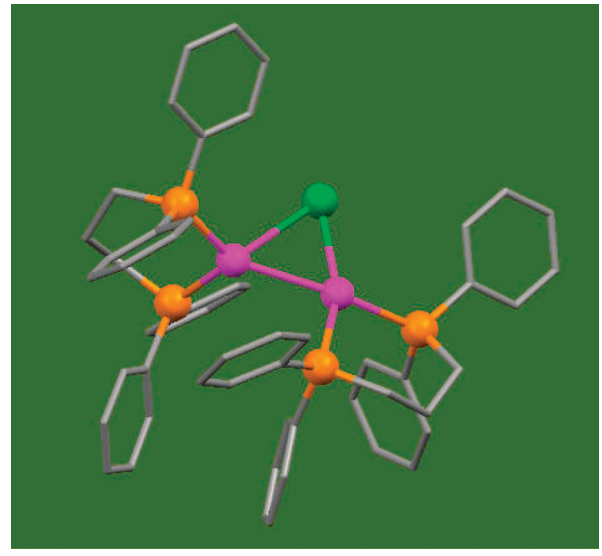

Figure 6. Chelate structure of $[Au_2(DPPP)_2Cl]^+$ obtained with DFT methods and having H atoms omitted for clarity. P, orange; C, gray; H, white; Au, purple; and Cl, green.

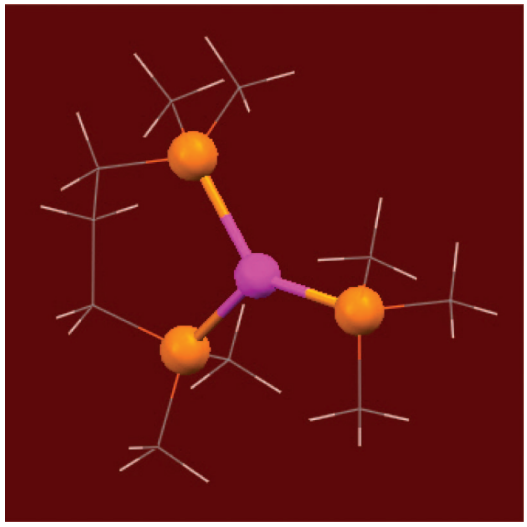

Figure 7. Geometry-optimized triangular $[Au^{I}(DMPP)(PMet_3)]^+$ complex. P, orange; C, gray; H, white; and Au, purple.

Scheme 5. A Modeled Hypochlorite Oxidation for Au(I) to Au(III)

$$[Au^{I}(DMPP)(PMet_3)]^+ + 2[H]^+ + 4[OCl]^- \rightarrow [Au^{III}Cl_4]^- + DMPPO_2 + PMet_3O + H_2O$$

is almost insignificant from a structural viewpoint, because the distances between the Au atom and the plane made by the three P atoms are 0.280 and 0.016 Å, respectively, that is, both complexes can be considered as 3-coordinate. Because $[Au(DPPP)(PPh_3)]^+$ is observed experimentally with NMR and ESI-MS, and its solubility is higher than that of $[Au(DPPP)(PPh)_3Cl]$ in biological fluids, we suggest that this cationic species may be the active drug; therefore, we modeled the redox process by using $[Au(DMPP)(PMet_3)]^+$ as starting material (see Scheme 5 and Figure 7). ΔG for this reaction is −126.7 kcal/mol and indicates thermodynamic feasibility.

Discussion

Melanoma is the most aggressive of skin tumors, and this disseminated disease is characterized by a very poor clinical outcome, not modified by conventional anticancer treatments.[30] New agents and novel approaches are under preclinical evaluation for this malignancy.[31] In this context, it has been shown that $[Au(DPPP)(PPh_3)Cl]$ is highly cytotoxic against several human tumor cell lines and displays a selective activity in melanoma cells.[19] This activity has been recently confirmed on other human tumor cells and demonstrated to be related to apoptosis induction associated with impairment of mitochondrial function.[20]

The aim of the present study was to assess the effect of shortening the bridge between PPh_2 units on the cytotoxicity, that is, modifying $-[(CH)_2]_3-$ to $-[(CH)_2]_2-$. The rationale for this synthesis was also supported by the fact that less lipophilic phosphines are more tumor-selective and induce fewer side effects in their Au chelates.[32]

Applying the same synthetic route[19] used for $[Au(DPPP)(PPh_3)Cl]$ gave crystalline $[\{AuCl(PPh_3)\}_2(\mu_2\text{-DIPHOS})]$ as proven by diffraction methods; this compound was chemically characterized with IR spectroscopy, NMR, ESI-MS, and elemental analyses. The X-ray crystal structure of $[\{AuCl(PPh_3)\}_2(\mu_2\text{-DIPHOS})]$ shows a nonchelating DIPHOS ligand linking two Au centers. Therefore, the metal is 3-coordinate, that is, bound to one Cl and two P atoms, one from PPh_3 and one from DIPHOS. Considering that (a) DIPHOS induces a lower bite angle than DPPP and (b) the tendency of Au(I) to stabilize low coordination numbers (2 or 3 are more favorable than 4), we suggest that in combination the formation of a nonchelating species is induced; this is statistically favored as seen in the literature (Figure 2).

In JR8, SK-MEL-5, and the melanoma clone 2/60 cell lines, the in vitro cytotoxicity of $[\{AuCl(PPh_3)\}_2(\mu_2\text{-DIPHOS})]$ shows higher IC_{50} values (1.5 times or more) than those reported for $[Au(DPPP)(PPh)_3Cl]$.[20] Therefore, we performed a comparative study in solution for both species to determine a possible explanation for the systematic difference in activity. Because $[Au(DPPP)(PPh_3)Cl]$ undergoes partial dissociation in solution to several compounds, including the cytotoxic agent $[Au(DPPP)_2]^+$, the resulting variety may help increase the possibility of transporting DPPP to the target (Scheme 2). One of these compounds is the novel cationic species $[Au_2(DPPP)_2Cl]^+$, the equivalent of which was not detected for $[\{AuCl(PPh_3)\}_2(\mu_2\text{-DIPHOS})]$. Its structural features were investigated with DFT methods that gave the following observations: (a) a nonchelating connectivity having a Cl-bridged structure (Figure 5) and (b) an alternative connectivity having two $Au(DPPP)_2$ chelate moieties bridged by a Cl atom, depicted in Figure 6, with an Au−Au separation of 2.711 Å, thus showing a stronger aurophilic interaction compared to that of related crystalline compounds having the same Au−Cl−Au moiety.

Therefore, by shortening the distance between both PPh_2 groups (by using DIPHOS instead of DPPP), a different Au complex is stabilized; this complex has a unique triangular Au coordination and a nonchelating structure with Au−P bonds weaker than those of the related nonchelate Au−DIPHOS compounds. Because a chelating ligand establishes stronger metal binding than a nonchelating one, the latter complex is less stable, possibly explaining the lower activity than that observed for $[Au(DPPP)(PPh_3)Cl]$. This structure−activity relationship suggests a straightforward test on the crystal structures of other potential Au(I)−diphosphines; a strong Au−P binding favors diphosphine metal protection and increases access to the target. To check this hypothesis, we performed additional tests for both Au compounds on the B16V murine melanoma cell line. From dose−response curves following 48 h of exposure to $[Au(DPPP)(PPh_3)Cl]$ and $[\{AuCl(PPh_3)\}_2(\mu_2\text{-DIPHOS})]$, IC_{50} values of 0.09 and 0.32 μM were obtained, respectively. These results confirm that the nonchelate complex $[\{AuCl(PPh_3)\}_2(\mu_2\text{-DIPHOS})]$ has a weaker activity than the chelate complex $[Au(DPPP)(PPh_3)Cl]$. The activity of both complexes in the B16V panel is about 10 times higher than in JR8, SK-MEL-5, and 2/60 cell lines.

The mechanism of action of Au(I)−diphosphine derivatives is still largely unknown. Au seems to function as a carrier for the diphosphine ligand which can be displaced, for example, by thiol groups reacting with Au(I). The resulting free diphospines are able to function as antiproliferative agents.[33−35] However, a more direct involvement of Au in antitumor activity is feasible, because some Au(III) compounds, without any phosphine bound to the metal, are also active against several tumor models.[36] Potential explanations may come from clinically used antiarthritic Au(I) drugs, because they do not cause the release of peptide from human leukocyte antigen (HLA-DR1) in vitro, but the Au(III) square-planar compound $K[AuCl_4]$ releases peptides from HLA-DR4,[37] which are frequently found in individuals with rheumatoid arthritis; these features were also analyzed for other isoelectronic square-planar complexes (cis-

platin and $K_2[PdCl_4]$). Oxidation of Au(I) to Au(III) has been reported in vivo[38] and in vitro,[39] and Au(III) metabolites formed in vivo are responsible for severe allergic side effects from Au therapy. In addition, Au(I) pharmaceuticals are considered prodrugs that convert to Au(III) after interaction with hypochlorite produced by phagocytes.[26] By using spectroscopic NMR and ESI-MS of solution chemistry, we show that, upon addition of hypochlorite to [Au(DPPP)(PPh_3)Cl], there is oxidation to $[AuCl_4]^-$, $DPPPO_2$, and PPh_3O. A DFT investigation that includes structural calculations of these compounds shows a related oxidation reaction having thermodynamic feasibility.

Conclusions

The confirmation of chelating diphosphines as a necessary feature for effective antitumor activity in their Au(I) derivatives is shown by [Au(DPPP)(PPh_3)Cl] being more effective than [{AuCl(PPh_3)}$_2$(μ_2-DIPHOS)] against melanoma. [Au(DPPP)(PPh_3)Cl] decomposition in solution includes the novel cation $[Au_2(DPPP)_2Cl]^+$, the biological role of which is not clear at present. In addition, redox interaction of [Au(DPPP)(PPh_3)Cl] with the endogenous hypochlorite anion leads to the corresponding square-planar $[AuCl_4]^-$ and phosphine oxidation; DFT shows this reaction to be thermodynamically favorable and perhaps related to the antitumor mechanism of action.

Experimental Section

Chemistry. DIPHOS, DPPP, and (PPh_3)AuCl were purchased from Aldrich and used without further purification. All solvents were dried, degassed, and distilled prior to use. Elemental analyses (C, H) were performed with a Fisons Instruments 1108 CHNS-O elemental analyzer. Buffer solution (Fluka): pH 9.0 (20.0 °C) sodium tetraborate (borax/hydrochloric acid); pH 5.0 (20 °C) sodium citrate. IR spectra were recorded from 4000 to 100 cm^{-1} with a Perkin-Elmer System 2000 FTIR instrument. ^1H and $^{31}P\{^1H\}$ NMR spectra, referenced to $Si(CH_3)_4$ and external 85% H_3PO_4, respectively, were recorded on a VXR-300 Varian spectrometer (300 MHz for ^1H and 121.4 MHz for ^{31}P). Relative intensity of signals is given in square brackets and *J* in hertz. The interaction of [Au(DPPP)(PPh_3)Cl] with hypochlorite was studied with ^1H and ^{31}PNMR spectra recorded on a Mercury Plus Varian 400 NMR spectrometer (400 MHz for ^1H and 162.1 MHz for ^{31}P). Positive and negative electrospray mass spectra were obtained with a Series 1100 MSI detector HP spectrometer by using an acetonitrile mobile phase. Solutions (3 mg/mL) for ESI-MS were prepared by using reagent grade acetonitrile. For the ESI-MS data, masses and intensities were compared to those calculated by using the IsoPro Isotopic Abundance Simulator, version 2.1;[40] peaks containing chloride are identified as the centers of isotopic clusters.

Chloro-triphenylphosphine-1,3-bis(diphenylphosphino)propane-gold(I). [Au(DPPP)(PPh_3)Cl] was synthesized as previously reported.[19] IR (Nujol mull, cm^{-1}): 3060w, 3039w, 1990w, 1906w, 1826w, 1770w, 1671w, 1582m, 1569m, 1436m, 1313m, 1196br, 1094s, 1070w, 1043w, 1026w, 998w, 971m, 824m, 794m, 761m, 747m, 738m, 722m, 710m, 697s, 648m, 617w, 547m, 530m, 515s, 508s, 491m, 470m, 429m, 398w, 357w, 329w, 302w, 280w, 252sh, 248w, 227w. ^1H NMR ($CDCl_3$, 295 K, δ ppm): 2.2br (CH_2, 2H), 2.6br (CH_2, 4H), 7.0–7.7m br (CHPh, 35H). ^{31}P NMR (DMSO, 293 K, δ ppm): 0.11br [10], 26.6br [1], 31.0 [2], 31.7br [10], 34.62br [30]. ^{31}P NMR (CDCl3, 293 K, δ ppm): −1.7br [1], 26.4br [1], 32.7br [1].

The $^{31}P\{^1H\}$ NMR spectrum of [Au(DPPP)(PPh_3)Cl], taken at room temperature in $CDCl_3$, shows three signals that can be assigned to the two different phosphorus environments in the complex (PPh_3 and DPPP) and to $[Au(DPPP)_2]Cl$. Some minor signals appear after 30 min because of free PPh_3 and $[Au(PPh_3)_2Cl]$, suggesting partial dissociation of the complex in this solvent. A similar behavior has been displayed in DMSO, where the predominant species are $[Au(DPPP)_2]Cl$, $[Au(DPPP)PPh_3Cl]$, and $[Au(PPh_3)_2Cl]$.

To confirm the dissociation equilibrium in solution of [Au(DPPP)(PPh_3)Cl], an ESI-MS study was carried out on its MeCN solutions at different concentrations. In the positive mode, the following cations were identified: $[Au(DPPP)(PPh_3)]^+$, $[Au(DPPP)_2]^+$, $[Au(PPh_3)_2]^+$, and $[Au_2(DPPP)_2]Cl^+$, with the latter three species being less abundant.

ESI-MS (MeCN): (+) 721.5 [10] $[(PPh_3)_2AuCl]^+$, 871.7 [80] $[Au(DPPP)(PPh_3)]^+$, 1021.8 [100] $[Au(DPPP)_2]^+$, 1253.8 [5] $[Au_2(DPPP)_2]Cl]^+$. Therefore, by combining ESI-MS and NMR spectra, it is demonstrated that this compound undergoes partial dissociation in $CHCl_3$, DMSO, and MeCN, yielding stable and known species and the novel cationic species $[Au_2(DPPP)_2]Cl^+$.

Interaction of [Au(DPPP)(PPh_3)Cl] with Hypochlorite. ^{31}P NMR ($CDCl_3$, 293 K, δ ppm): 16.5s [10], 27.8s [2], 28.2s [1], 29.2 [2], 30.6 [10], 33.5d [2] (82 Hz), 34.1 [5], 34.2 [10], 41.1d [2] (44 Hz), 41.9 [2], 45.0 [2]. ^1H NMR (CD_2Cl_2, 293 K, δ ppm): 1.9 br (2H, CH_{2DPPP}), 1.9 br (2H, CH_{2DPPP}), 2.7 br (4H, CH_{2DPPP}), 7.0−8.0 (35H, $CH_{PPh3\ +\ DPPP}$).

ESI-MS (MeCN, 25 °C): (−) 338.8 [100] ($AuCl_4^-$), 266.9 [40] ($AuCl_2^-$). (+) 911 [100] ($(DPPPO_2)_2 + Na^+$), 745 [40] $[(PPh_3O)(DPPPO_2) + Na]^+$, 679 [65] $[(DPPP)AuCl_2]^+$, 529 [25] $[(PPh_3)AuCl_2]^+$, 445 [80] $[(DPPPO_2) + H]^+$.

Bis(chloro-triphenylphosphinegold(I))-μ^2-1,2-bis(diphenylphosphino)ethane. Because crystalline [Au(DPPP)(PPh_3)Cl] was obtained from slow evaporation of [Au(PPh_3)Cl] and DPPP in dichloromethane (1:1 ratio),[19] we mixed [Au(PPh_3)Cl] and DIPHOS accordingly. Crystalline material from chloroform solutions was obtained; unexpectedly, diffraction methods showed it to be [{AuCl(PPh_3)}$_2$(μ_2-DIPHOS)]. When we tried the same 1:1 ratio in diethyl ether, $[(DIPHOS)_2Au]^+$ formed, that is, a different product than obtained from chloroform. However, reacting [Au(PPh_3)Cl] and DIPHOS (2:1) in diethyl ether yielded [{AuCl(PPh_3)}$_2$(μ_2-DIPHOS)], as reported above for chloroform. That is, upon addition of 0.41 g of DIPHOS (ca. 1.0 mmol) to a suspension (50 mL) of [Au(PPh_3)Cl] (1.00 g, ca. 2.0 mmol) in diethyl ether, a colorless precipitate formed. The suspension was then stirred for 4 h and filtered, and the precipitate was washed with diethyl ether (20 mL) to give 0.70 g (0.5 mmol, 50%) of the title compound, mp 189−191 °C. Anal. ($C_{62}H_{54}Au_2Cl_2P_4$) C, H. IR (Nujol mull, cm^{-1}): 3050w, 3020w, 1585w, 1572w, 545m, 532m, 515s, 508s, 492s, 454m. ^1H NMR ($CDCl_3$): δ 2.5 (br, 2H, CH_2), 3.0 (br, 2H, CH_2), 7.2−7.8 (m, 50H, C_6H_5). ^{31}P NMR ($CDCl_3$): 21.14, 33.35, 34.55. ESI-MS (+) (CH_3CN): 721.5 (30) $[(PPh_3)_2Au^+]$, 857.5 (40) $[(PPh_3)(DIPHOS)Au^+]$, 993.8 (100) $[(DIPHOS)_2Au^+]$, 1090 (20) $[(PPh_3)(DIPHOS)Au_2Cl^+]$, 1352 (10) $[(PPh_3)_2(DIPHOS)Au_2Cl^+]$, 1457 (5) $[(DIPHOS)_2Au_3Cl_2^+]$. When different molar ratios were employed, for example Au(PPh_3)Cl:DIPHOS (1:1) or Au(PPh_3)Cl:DIPHOS (1:2), the well-known [Au (DIPHOS)$_2$]Cl formed.

X-ray Study of [{AuCl(PPh_3)}$_2$(μ_2-DIPHOS)]. Very slow evaporation of this compound in chloroform solution afforded plate-shaped crystals. A preliminary Weissenberg study showed cell parameters and space group. The crystal was placed in a quartz capillary to attenuate the strong and anisotropic decay. The molecular structure was determined with the Patterson function and successive Fourier localizations by using CAOS program.[41] The obtained high R_f is probably due to anisotropic crystal decay. The molecule is centro-symmetric, and the inversion center is located halfway along the ethylene bridge. The asymmetric unit is half a molecule plus $CHCl_3$, so that the crystalline compound is formally [{AuCl(PPh_3)}$_2$(μ_2-DIPHOS)]·2$CHCl_3$. Table S4 shows crystallographic data.

Theoretical Study. The structural features of the novel cationic species $[Au_2(DPPP)_2Cl]^+$ were analyzed with DFT by using the Accelrys program Cerius2 4.6, subroutine DMol3 on an Octane SGI computer.[42] Reliability of this program was already observed in performing structural calculations on related compounds.[43] Because of the large scale calculations, an electron−core potential technique was employed. Local density was the Perdew and Wang functional[44] using a double numeric basis set with polarization functions (DNP)[45] on all atoms. Initial coordinates for a nonchelate arrangement of $[Au_2(DPPP)_2Cl]^+$ (Scheme 4, left) were obtained

after modification of the closely related bis(μ_2-chloro)-bis(μ_2-*R*,*S*-(1-diphenylphosphinobut-2-yl)-diphenylphosphinite)-digold(I) crystal structure,[29] which has two Cl atoms bridging the two metal centers and a C−C−O link between the two PPh_2 moieties. Therefore, this link was updated to $-(CH_2)_3-$, and one Cl atom was excluded. To ensure obtaining an absolute energy minimum, discrete modifications of the initial structure were performed; all of them converged to the same geometry, see Figure 5. The Au−Au separation of 4.441 Å is slightly longer than the one from which the structure was modeled (4.338 Å). Cartesian coordinates of the converged structure are presented in the Supporting Information (Table S1). Au(I) shows a marked preference for the coordination number 2, and an alternative configuration without the Cl bridge was also explored. In this arrangement, one Au atom is 3-coordinate and bound to one Cl and two P atoms, and the other Au atom is 2-coordinate and bound to two P atoms. Several models of this type did not reach convergence, and their minimization paths became erratic. Also, structures obtained by using these pathways showed energy markedly higher than that of the bridged structure, and we conclude that the Au−Cl−Au bridged cation is preferred to the one having a terminal Cl.

An alternative connectivity having two chelating Au(DPPP) moieties linked by a Cl atom was also explored (Scheme 4, right). The coordinates of the flexible trimethylene bridge and the phenyls were widely varied to avoid trapping in non-absolute minima. The best converged molecule has a Au−Cl−Au moiety typical of aurophilic interaction and is shown in Figure 6; related coordinates are also presented in the Supporting Information (Table S2). The same DMol3 conditions were used to refine the molecular structure of the crystalline [{AuCl(PPh_3)}$_2$(μ_2-DIPHOS)] species.

Calculations for oxidation of [Au(DPPP)(PPh_3)Cl] to $[AuCl_4]^-$, PPh_3O, and $DPPPO_2$ were performed by using DMol3 as implemented in the program Materials Studio 4.0 (PC version) by using a BP/DNP basis set closely related to that used in the SGI platform and including relativistic effects for the metal.

Biological Study. Cell Lines. Human melanoma cell lines, JR8 and SK-MEL-5, and the melanoma clone 2/60 (selected from the human melanoma cell line 665/2 by micromanipulation in soft agar) were compared to related data.[20] The biological characteristics of JR8, SK-MEL-5, and 2/60 have been previously described.[46,47] Cell lines were maintained in logarithmic growth phase at 37 °C in a 5% CO_2 humidified atmosphere in air. RPMI-1640 medium (Biowhittaker, Verviers Industries, Kibbutz Beth Haemek, Israel) containing 10% fetal calf serum, 2 mM L-glutamine, and 0.1 mg/mL gentamycin was used for all cell lines. For these cell lines, the experiments were performed within 10 passages from thawing. An additional test in vitro was performed for both compounds in the B16V cell line. This murine model, an in vitro line derived from the in vivo transplanted B16 melanoma, was a gift from Dr. R. Supino (Istituto Nazionale Tumori, Milan, Italy).[48] Cells were maintained in RPMI-1640 medium (Sigma-Aldrich, Milan, Italy), supplemented with 10% fetal bovine serum (Celbio, Italy), 2 mM glutamine, 1% antibiotic mixture, and 0.03 mM $K_3Fe(CN)_6$ at 37 °C in a humidified 5% CO_2 atmosphere.

Drugs. [{AuCl(PPh_3)}$_2$(μ_2-DIPHOS)] was reconstituted in sterile DMSO at a concentration of 5 mM and then diluted with sterile water to the desired concentrations, immediately before each experiment, for JR8, SK-MEL-5, the melanoma clone 2/60, and B16V cell lines. The same technique was applied for [Au(DPPP)(PPh_3)Cl] in the B16V cell line.

Cell Survival Assay. The sulforhodamine B (SRB) assay was performed on all the cell lines tested as described[49] with minor modifications. Briefly, according to the growth profiles previously defined for each cell line, adequate numbers of cells in 0.2 mL culture medium were plated in each well of a 96-well plate and allowed to attach for 24 h. Cells were exposed at 37 °C for 48 h to different concentrations of the two Au complexes ranging between 0.1 and 1000 μM for the human melanoma cell lines or between 0.01 and 10 μM for B16V cells. Each experiment included eight replications for each concentration tested; control samples were run with 0.2% DMSO. At the end the 48 h period of incubation with the Au complexes, cells were fixed and processed for SRB staining. The optical density was read at 550 nm by using a Universal Microplate Reader EL800 (Bio-Tek Instruments, Winooski, VT), and the results were expressed as cell growth obtained from the ratio of the absorbance values of Au-complex-treated samples and those of controls. Dose−response curves were analyzed by nonlinear regression analysis, and IC_{50} values were estimated by using GraphPad Prism software, v. 4.03. The in vitro activity of the drugs was expressed as IC_{50} (i.e., the concentration inhibiting cell proliferation by 50%).

Acknowledgment. The authors acknowledge the Università di Camerino, Fondazione Carima, and Vassar College Research Committee and Cristian Opazo at Vassar College SCIVIS lab for support with DMol3 program.

Supporting Information Available: DFT molecular coordinates for chelate (Table S1) and nonchelate (Table S2) converged structures of $[Au_2(DPPP)_2Cl]^+$ and for [{AuCl(PPh_3)}$_2$(μ_2-DIPHOS)] (Table S3). X-ray data, fractional coordinates, and displacement parameters of [{AuCl(PPh_3)}$_2$(μ_2-DIPHOS)] (Tables S4−S6). Full lists of X-ray bond distances and angles for [{AuCl(PPh_3)}$_2$(μ_2-DIPHOS)] (Tables S7−S8). List of Au−DIPHOS chelate ref codes for 3-coordinate metal found in the CSD (Table S9). DFT drawing of [{AuCl(PPh_3)}$_2$(μ_2-DIPHOS)] (Figure S1). This material is available free of charge via the Internet at http://pubs.acs.org.

References

(1) Zhang, C. X.; Lippard, S. J. New metal complexes as potential therapeutics. *Curr. Opin. Chem. Biol.* **2003**, *7*, 481–489.
(2) Guo, Z.; Sadler, P. J. Medicinal inorganic chemistry. *Adv. Inorg. Chem.* **2000**, *49*, 183–306.
(3) Shaw, C. F., III. Gold-based therapeutic agents. *Chem. Rev.* **1999**, *99*, 2589–2600.
(4) Tiekink, E. R. T. Gold derivatives for the treatment of cancer. *Crit. Rev. Oncol. Hematol.* **2002**, *42*, 225–248.
(5) Simon, T. M.; Kunishima, D. H.; Vibert, G. J.; Lorber, A. Screening trial with the coordinated gold compound auranofin using mouse lymphocytic leukemia P388. *Cancer Res.* **1981**, *41*, 94–97.
(6) Mirabelli, C. K.; Johnson, R. K.; Sung, C.-M.; Faucette, L. F.; Muirheard, K.; Crooke, S. T. Evaluation of the in vivo antitumor activity and in vitro cytotoxic properties of Auranofin, a coordinated gold coumpound, in murine tumor models. *Cancer Res.* **1985**, *45*, 32–39.
(7) Mirabelli, C. K.; Johnson, R. K.; Hill, D. T.; Faucette, L. F.; Girard, G. R.; Kuo, G. Y.; Sung, C.-M.; Crooke, S. T. Correlation of the *in vitro* cytotoxic and *in vivo* antitumor activities of Gold (I) coordination complexes. *J. Med. Chem.* **1986**, *29*, 218–223.
(8) Berners-Price, S. J.; Girard, G. R.; Hill, D. T.; Sutton, B. M.; Jarret, P. S.; Faucette, L. F.; Johnson, R. K.; Mirabelli, C. K.; Sadler, P. J. Cytotoxicity and antitumor activity of some tetrahedral bis. (diphosphino)gold(I) chelates. *J. Med. Chem.* **1990**, *33*, 1386–1392.
(9) Rigobello, P.; Messori, L.; Marcon, G.; Cinellu, A. M.; Bragadin, M.; Folda, A.; Scutari, G.; Bindoli, A. Gold complexes inhibit mitochondrial thioredoxin reductase: Consequences on mitochondrial functions. *J. Inorg. Biochem.* **2004**, *98*, 1634–1641.
(10) Rigobello, P.; Scutari, G.; Folda, A.; Bindoli, A. Mitochondrial thioredoxin reductase inhibition by gold(I) compounds and concurrent stimulation of permeability transition and release of cytochrome c. *Biochem. Pharmacol.* **2004**, *67*, 689–696.
(11) Hoke, G. D.; Rush, G. F. Mechanism of alterations in isolated rat liver mitochondrial function induced by gold complexes of bidentate phosphines. *J. Biol. Chem.* **1988**, *263*, 11203–11210.
(12) Barnard, P. J.; Baker, M. V.; Berners-Price, S. J.; Day, D. A. Mitochondrial permeability transition induced by dinuclear gold(I)-carbene complexes: Potential new antimitochondrial antitumour agents. *J. Inorg. Biochem.* **2004**, *98*, 1642–1647.
(13) McKeage, M. J. Gold opens mitochondrial pathways to apoptosis. *Br. J. Pharmacol.* **2002**, *136*, 1081–1082.
(14) Ly, J. D.; Grubb, D. R.; Lawen, A. The mitochondrial membrane potential (deltapsi. (m)) in apoptosis; An update. *Apoptosis* **2003**, *8*, 115–128.
(15) Zhou, L. L.; Zhou, L. Y.; Luo, K. Q.; Chang, D. C. Smac/DIABLO and cytochrome c are released from mitochondria through a similar mechanism during UV-induced apoptosis. *Apoptosis* **2005**, *10*, 289–299.

(16) Garber, K. Targeting mitochondria emerges as therapeutic strategy. *J. Natl. Cancer Inst.* **2005**, *97*, 1800–1801.
(17) Bras, M.; Queenan, B.; Susin, S. A. Programmed cell death via mitochondria: Different modes of dying. *Biochemistry* **2005**, *70*, 231–239.
(18) Mohamad, N.; Gutierrez, A.; Nunez, M.; Cocca, C.; Martin, G.; Cricco, G.; Medina, V.; Rivera, E.; Bergoc, R. Mitochondrial apoptotic pathways. *Biocell* **2005**, *29*, 149–161.
(19) Caruso, F.; Rossi, M.; Tanski, J.; Pettinari, C.; Marchetti, F. Antitumor activity of the mixed phosphine gold species chlorotriphenylphosphine-1,3-bis. (diphenylphosphino)propanegold(I). *J. Med. Chem.* **2003**, *46*, 1737–1742.
(20) Caruso, F.; Villa, R.; Rossi, M.; Pettinari, C.; Paduano, F.; Pennati, M.; Daidone, M. G.; Zaffaroni, N. Mitochondria are primary targets in apoptosis induced by the mixed phosphine gold species chlorotriphenylphosphine-1,3-bis. (diphenylphosphino)propanegold(I) in melanoma cell lines. *Biochem. Pharmacol.* **2006**, *6*, 773–781.
(21) Schmidbaur, H.; Dziwok, K.; Grohmann, A.; Mueller, G. Further evidence for attractive interactions between gold(I) centers in binuclear complexes. *Chem. Ber.* **1989**, *122*, 893–895.
(22) (a) Elder, R. C.; Zeiher, E. H. K.; Onady, M.; Whittle, R. R. Nearly regular tetrahedral geometry in a gold(I)-phosphine complex. X-ray crystal structure of tetrakis. (methyldiphenylphosphine)-gold(I) hexafluorophosphate. *J. Chem. Soc., Chem. Commun.* **1981**, 900–901. (b) Jones, P. G. Is Regular tetrahedral geometry possible in gold(I)-phosphine complexes? X-ray crystal structure of three modifications of $[(PPh_3)_4Au][BPh_4]$. *J. Chem. Soc., Chem. Commun.* **1980**, 1031–1033. (c) Parish, R. V.; Rush, J. D. Gold-197 Mössbauer spectra of two-, three-, and four-coordinate gold(I) complexes. *Chem. Phys. Lett.* **1979**, *63*, 37–39. (d) Mays, M. J.; Vergnano, P. A. Structure and bonding in gold(I) compounds. A phosphorus-31 nuclear magnetic study of the structure of some gold(I) phosphine complexes in solution. *J. Chem. Soc., Dalton Trans.* **1979**, 1112–1115. (e) Colburn, C. B.; Hill, W. E.; McAuliffe, C. A. ^{31}P NMR study of tertiary phosphine complexes of gold(I). *J. Chem. Soc., Chem. Commun.* **1979**, 218–219. (f) Parish, R. V.; Parry, O.; McAuliffe, C. A. Characterization of two-, three, and four-coordinate gold-(I) complexes by 197Au Mö ssbauer and ^{31}P-$\{^1H\}$ nuclear magnetic resonance spectroscopy. *J. Chem. Soc., Dalton Trans.* **1981**, 2098–2104. (g) Muir, J. A.; Muir, M. M.; Arias, S.; Campana, C. F.; Dwight, S. K. Structure of the monoclinic form of thiocyanato tris. (triphenylphosphine)gold(I) monohydrate. *Acta Crystallogr.* **1982**, *38B*, 2047–2049. (h) Uson, R.; Laguna, A.; Vicente, J.; Garcia, J.; Jones, P. G.; Sheldrick, G. M. Preparation of three- and four-coordinate gold(I) complexes: crystal structure of bis[*o*-phenylenebis. (dimethylarsine)]gold(I) bis. (pentafluorophenyl)aurate(I). *J. Chem. Soc., Dalton Trans.* **1981**, 655–657. (i) Muir, J. A.; Muir, M. M.; Arias, S.; Jones, P. G.; Sheldrick, G. M. The crystal and molecular structure of the orthorhombic form of thiocyanato tris. (triphenylphosphine)gold(I) monohydrate $[(Ph_3P)_3Au(SCN)]$. H_2O. *Inorg. Chim. Acta* **1984**, *81*, 169–174.
(23) (a) Bates, P. A.; Waters, J. M. A tetrahedral complex of gold(I). The crystal and molecular structure of $Au(Ph_2PCH_2CH_2PPh_2)_2$-$Cl.2H_2O$. *Inorg. Chim. Acta* **1984**, *81*, 151–154. (b) Berners-Price, S. J.; Mazid, M. A.; Sadler, P. J. Stable gold(I) complexes with chelate rings: Solution studies of bis. (phosphino) ethane complexes and X-ray crystal structure of bis[1,2-bis. (diphenylphosphino)ethane] gold(I) hexafluoroantimoniate-acetone (1/1). *J. Chem. Soc., Dalton Trans.* **1984**, *96*, 9–974. (c) Berners-Price, S. J.; Brevard, C.; Pagelot, A.; Sadler, P. J. Cu-$(Ph_2PCH_2CH_2PEt_2)_2Cl$: a chelated copper(I) complex with tetrahedral stereochemistry. Rate of inversion compared with those of isostructural silver(I) and gold(I) complexes. *Inorg. Chem.* **1986**, *25*, 596–599. (d) Berners-Price, S. J.; Sadler, P. J. Gold(I) complexes with bidentate tertiary phosphine ligands: Formation of annular vs tetrahedral chelated complexes. *Inorg. Chem.* **1986**, *25*, 3822–3827. (e) Berners-Price, S. J.; Jarret, P. S.; Sadler, P. J. 31P NMR studies of $[Au_2(\mu\text{-dppe})]^{2+}$ antitumor complexes. Conversion into $[Au.(dppe)_2]^+$ induced by thiols and blood Plasma. *Inorg. Chem.* **1987**, *26*, 3074–3077.
(24) (a) Barranco, E. M.; Crespo, O.; Gimeno, M. C.; Laguna, A.; Jones, P. G.; Ahrens, B. Gold and silver complexes with the ferrocenyl phosphine $FcCH_2PPh_2$ [Fc = $(\eta^5\text{-}C_5H_5)Fe(\eta^5\text{-}C_5H_4)$]. *Inorg. Chem.* **2000**, *39*, 680–687. (b) Bardajı′, M.; Laguna, A.; Orera, V. M.; Villacampa, M. D. Synthesis, structural characterization, and luminescence studies of gold(I) and gold(III) complexes with a triphosphine ligand. *Inorg. Chem.* **1998**, *37*, 5125–5130. (c) Bardajı′, M.; Laguna, A.; Vicente, J.; Jones, P. G. Synthesis of luminescent gold(I) and gold(III) complexe with a triphosphine ligand. *Inorg. Chem.* **2001**, *40*, 2675–2681.
(25) Cooper, M. K.; Mitchell, L. E.; Henrick, K.; McPartlin, M.; Scott, M. The synthesis and X-ray structure analysis of dichloro{1,3-bis. (diphenylphosphino)propane}digold(I). *Inorg. Chim. Acta* **1984**, *84*, L9–L10.
(26) Babior, B. M.; Kipnes, R. S.; Curnutte, J. T. Biological defense mechanisms. The production by leukocytes of superoxide, a potential bactericidal agent. *J. Clin. Invest.* **1973**, *52*, 741–744.
(27) Attar, S.; Nelson, J. H.; Bearden, W. H.; Alcock, N. W.; Solujic, L.; Milosavljevic, E. B. Phosphole complexes of gold(III) halides: Synthesis, structure, electrochemistry and ligand redistribution reactions. *Polyhedron* **1991**, *10*, 1939–1949.
(28) Serafimova, I. M.; Hoggard, P. E. The photochemistry of chloro. (triphenylphosphine)gold(I) and trichlorotriphenylphosphine)gold(III) in chloroform. *Inorg. Chim. Acta* **2002**, *338*, 105–110.
(29) Bayler, A.; Schier, A.; Schmidbaur, H. Four-coordinate gold(I), silver(I), and copper(I) complexes with a large-span chiral ditertiary phosphine ligand. *Inorg. Chem.* **1998**, *37*, 4353–4359.
(30) Thompson, J. F.; Scolyer, R. A.; Kefford, R. F. Cutaneous melanoma. *Lancet* **2005**, *365*, 687–701.
(31) Grossman, D.; Altieri, D. C. Drug resistance in melanoma: mechanisms apoptosis and new potential therapeutic targets. *Cancer Metastasis Rev.* **2001**, *20*, 3–11.
(32) Berners-Price, S. J.; Bowen, R. J.; Galettis, P.; Healy, P. C.; McKeage, M. J. Structural and solution chemistry of gold(I) and silver(I) complexes with bidentate pyridil phosphines: Selective antitumor agents. *Coord. Chem. Rev.* **1999**, *185–186*, 823–826.
(33) Mirabelli, C. K.; Hill, D. T.; Faucette, L. F.; McCabe, F. L.; Girard, G. R.; Bryan, D. B.; Sutton, B. M.; Barus, J. O.; Crooke, S. T.; Johnson, R. K. Antitumor activity of bis. (diphenylphosphino)alkanes, their gold(I) coordination complexes, and related compounds. *J. Med. Chem.* **1987**, *30*, 2181–2190.
(34) Berners-Price, S. J.; Mirabelli, C. K.; Johnson, R. K.; Mattern, M. R.; McCabe, F. L.; Faucette, L. F.; Sung, C.-M.; Mong, S.-M.; Sadler, P. J.; Crooke, S. T. In vivo antitumor activity and in vitro cytotoxic properties of bis[1,2-bis. (diphenylphosphino)-ethane]gold(I) chloride. *Cancer Res.* **1986**, *46*, 5486–5493.
(35) Struck, R. F.; Shealy, Y. F. Tertiary phosphines and phosphine oxides containing a 2-haloethyl group. *J. Med. Chem.* **1966**, *9*, 414–416.
(36) Ronconi, L.; Marzano, C.; Zanello, P.; Corsini, M.; Miolo, G.; Macca, C.; Trevisan, A.; Fregona, D. Gold (III) dithiocarbamate derivatives for the treatment of cancer: Solution chemistry, DNA binding, and hemolytic properties. *J. Med. Chem.* **2006**, *49*, 1648–1657.
(37) De Wall, S. L.; Painter, C.; Stone, J. D.; Bandaranayake, R.; Wiley, D. C.; Mitchison, T. J.; Stern, L. J.; DeDecker, B. S. Noble metals strip peptides from class II MHC proteins. *Nat. Chem. Biol.* **2006**, *2*, 197–201.
(38) Goebel, C.; Kubicka-Muranyi, M.; Tonn, T.; Gonzalez, J.; Gleichmann, E. Phagocytes render chemicals immunogenic: Oxidation of gold(I) to the T cell-sensitizing gold(III) metabolite generated by mononuclear phagocytes. *Arch. Toxicol.* **1995**, *69*, 450–459.
(39) Shaw, C. F., III.; Schraa, S.; Gleichmann, E.; Grover, Y. P.; Dunemann, L.; Jagarlamudi, A. Redox chemistry and $[Au(CN)_2]^-$ in the formation of gold metabolites. *Metal Based Drugs* **1994**, *1*, 351–362.
(40) Senko, M. W. IsoPro isotopic abundance simulator, v. 2.1; National High Magnetic Field Laboratory, Los Alamos National Laboratory: Los Alamos, NM.
(41) Camalli, M.; Spagna, R. CAOS program. *J. Appl. Crystallogr.* **1994**, *27*, 861–862.
(42) Delley, B. An all-electron numerical method for solving the local density functional for polyatomic molecules. *J. Chem. Phys.* **1990**, *92*, 508–517.
(43) Caruso, F.; Rossi, M.; Opazo, C.; Pettinari, C. Structural features of antitumor gold(I)-phosphine derivatives analyzed with theoretical methods. *J. Argen. Chem. Soc.* **2004**, *92*, 119–124.
(44) Perdew, J. P.; Chevary, J. A.; Vosko, S. H.; Jackson, K. A.; Pederson, M. R.; Singh, D. J.; Fiolhais, C. Atoms, molecules, solids, and surfaces: applications of the generalized gradient approximation for exchange and correlation. *Phys. Rev. B* **1992**, *46*, 6671–6687.
(45) Delley, B. Fast calculation of electrostatics in crystals and large molecules. *J. Phys. Chem.* **1996**, *100*, 6107–6110.
(46) Badaracco, G.; Corsi, A.; Maisto, A.; Natali, P. G.; Storace, G.; Zupi, G. Expression of tumor-associated antigens and kinetic profile of two melanoma cell lines. *Cytometry* **1981**, *2*, 63–69.
(47) Supino, R.; Mapelli, E.; Sanfilippo, O.; Silvestro, L. Biological and enzymatic features of human melanoma clones with different invasive potential. *Melanoma Res.* **1992**, *2*, 377–384.
(48) Formelli, F.; Rossi, C.; Supino, R.; Parmiani, G. In vivo characterization of a doxorubicin resistant B16 melanoma cell line. *Br. J. Cancer* **1986**, *54*, 223–33.
(49) Perez, R. P.; Godwin, A. K.; Handel, L. M.; Hamilton, T. C. A comparison of clonogenic, microtetrazolium and sulforodamine B assays for determination of cisplatin cytotoxicity in human ovarian carcinoma cell lines. *Eur. J. Cancer* **1993**, *29A*, 395–399.

JM700978A